engineering proceedings

MDPI

Proceeding Paper

Assessment of SoC Estimation Methods for a Fuel Cell/Battery Hybrid Electric Vehicle During the WLTP Driving Cycle †

Kübra Nur Akpınar [1,*], Buğra Yılmaz [2], Barış Çavuş [3] and Seçil Genç [3]

[1] Department of Electrical and Energy, Vocational School of Technical Sciences, Marmara University, Kartal, 34865 İstanbul, Türkiye
[2] School of Civil Aviation, Fırat University, 23119 Elazığ, Türkiye; b.yilmaz@firat.edu.tr
[3] Department of Electrical and Electronics Engineering, Ondokuz Mayıs University, Atakum, 55200 Samsun, Türkiye; baris.cavus@omu.edu.tr (B.Ç.); secil.yilmaz@omu.edu.tr (S.G.)
* Correspondence: knur@marmara.edu.tr
† Presented at the 8th International Conference on Nuclear and Renewable Energy Resources (NURER 2026), Almaty, Kazakhstan, 10–12 September 2026.

Abstract

Accurate state-of-charge (SoC) information is essential for the energy management of PEM fuel cell/battery hybrid electric vehicles (HEVs). This study examines how two SoC estimation approaches, Coulomb Counting (CC) and the Extended Kalman Filter (EKF), influence vehicle-level performance and internal power sharing under the same WLTP driving cycle and rule-based energy management strategy. Both methods yielded nearly identical vehicle-level performance, whereas the EKF produced a lower final SoC than CC (58.075% versus 60.902%) and greater SoC variability, indicating estimator-dependent differences in internal energy distribution. The findings are interpreted as estimator-dependent system behavior rather than a direct accuracy ranking.

Keywords: hybrid electric vehicle (HEV); PEM fuel cell; Li-ion battery; SoC estimation; Coulomb Counting; Extended Kalman Filter (EKF)

1. Introduction

One of the most crucial strategies to fight climate change and lower greenhouse gas emissions associated with reliance on fossil fuels is to electrify the transportation industry. Electric vehicles (EVs) have emerged as a desirable option in the automotive industry due to their technological and environmental advantages [1]. These vehicles include battery electric vehicles (BEVs), hybrid electric vehicles (HEVs), plug-in hybrid electric vehicles (PHEVs), fuel cell/battery hybrid electric vehicles (FCHEVs), and fuel cell electric vehicles (FCEVs), among others [2,3].

Among these technologies, both battery-based and hydrogen-based solutions play a crucial role in the transition toward low-carbon transportation. FCHEVs incorporate rechargeable batteries, with lithium-ion batteries (LIBs) widely regarded as the most promising option for next-generation electric vehicles due to their high energy density, long cycle life, and compact size [4]. In parallel, the role of hydrogen in transportation decarbonization has gained increasing importance in recent years [5–7]. In FCEVs, electrical energy is generated through the electrochemical reaction between hydrogen and oxygen, producing only water vapor as a byproduct. Among various fuel cell technologies, proton exchange membrane (PEM) fuel cells are considered the most suitable for transportation applications,

Check for updates

Academic Editors: Sümer Şahin, Hacı Mehmet Şahin and Bekir Dursun

Published: 23 October 2026

Copyright: © 2026 by the authors. Licensee MDPI, Basel, Switzerland. This article is an open access article distributed under the terms and conditions of the Creative Commons Attribution (CC BY) license.

owing to their high energy efficiency, low operating temperatures, and rapid start-up capability [8].

In order to optimize fuel efficiency and ensure the effective utilization of energy storage systems, hybrid energy management frameworks and coordinated control strategies are being developed [2]. However, as the share of renewable energy increases, the inherent intermittency and unpredictability of power generation can lead to mismatches between supply and demand, potentially causing grid instability. To mitigate these effects, energy storage systems, particularly batteries and hydrogen-based solutions, are widely employed to store excess energy and supply it when needed.

In this context, the effectiveness of energy management strategies is strongly dependent on the accurate monitoring and control of the battery state-of-charge (SoC). SoC directly influences energy distribution decisions between different sources, such as fuel cells and batteries, ensuring system efficiency, reliability, and longevity. Therefore, precise SoC estimation is a critical requirement for achieving optimal performance in both EVs and renewable energy storage systems [9]. To address the SoC estimation issue in the EV industry, researchers and industry professionals have investigated a number of strategies and techniques. These approaches include empirical models such as the open-circuit voltage method [10], the impedance-based method [11,12], the Kalman Filtering method [9] and the Coulomb Counting method. Unscented Kalman Filter (UKF) and AI-based methods are also used for SoC estimation. UKF can handle nonlinear battery behavior better, but it needs more computation. AI-based methods need large and representative datasets. This study focuses on CC and EKF to compare their effects on EMS behavior under the same conditions.

In this study, an FCHEV model was developed in MATLAB/Simulink 2023b to investigate the impact of SoC estimation on EMS and vehicle performance under different configurations. The influence of SoC estimation on KPIs, particularly energy consumption and system efficiency, was quantified under the same EMS strategy and WLTP driving profile. Two SoC methods, CC and EKF, were comparatively evaluated.

The novelty lies in systematically assessing SoC methods under identical conditions in a PEM FC/battery HEV. Unlike studies focusing solely on estimation accuracy, this work isolates the effect of SoC on EMS behavior. Results show that while vehicle-level metrics (speed tracking, power demand) remain largely unaffected, internal energy distribution and FC/battery power-sharing are significantly influenced, highlighting SoC as a critical factor in EMS decision-making and system behavior.

This paper is organized as follows: First, the Materials and Methods section describes the system configuration and presents the mathematical foundations of the EMS along with the CC and EKF methods used for SoC estimation. The second section presents the results, and the final section provides the overall conclusions.

2. Materials and Methods

The system created in the MATLAB Simulink environment, as shown in Figure 1, consists of a battery, DC-DC converters, a PEM fuel cell, an inverter, a control unit, and a BLDC motor connected to the drive system [13].

The EMS optimizes energy usage by monitoring and controlling power flow, using SoC data from the battery pack to manage electricity efficiently. In this study, Kalman Filtering and Coulomb Counting methods were compared to evaluate their impact on SoC prediction and overall system performance.

https://doi.org/10.3390/engproc2026160027

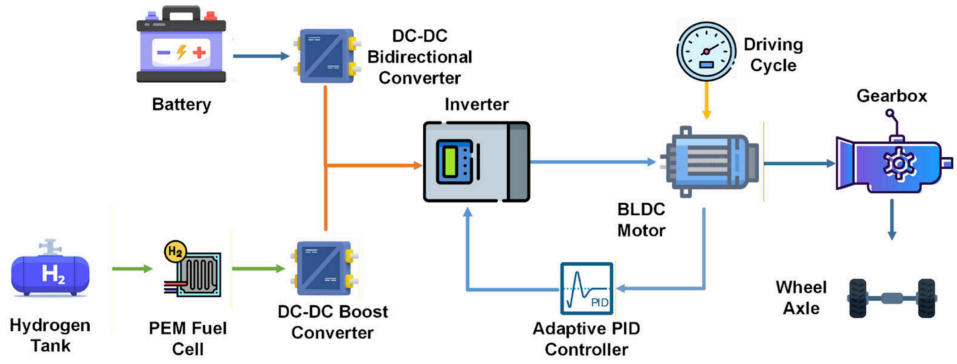


Figure 1. Block diagram of the system.

2.1. Energy Management System

The energy management strategy of the system is developed based on a rule-based logic framework with the primary objectives of maximizing the efficiency of the PEM Fuel Cell and ensuring the safe operation of system components. According to the flowchart illustrated in Figure 2, the control unit initially evaluates both environmental and internal parameters, including road slope, vehicle speed, and battery SoC, to determine the operating mode of the fuel cell. When the battery SoC exceeds a predefined threshold (SoC > 80%) or when the vehicle operates under negative slope conditions (downhill driving), regenerative operation is prioritized, and the fuel cell is switched to a passive mode to prevent unnecessary energy consumption. Conversely, when the vehicle speed exceeds a specified threshold (V > 25 km/h), a Perturb and Observe (P&O)-based Maximum Power Point Tracking (MPPT) algorithm is activated. In this stage, instantaneous variations in power (dP) and voltage (dV) are analyzed to continuously update the converter duty cycle, ensuring that the system operates at its maximum efficiency point under dynamic load conditions. To maintain system stability, the calculated duty cycle is constrained within predefined saturation limits, with a lower bound of 0.75 and an upper bound of 0.95, thereby generating the final control signal.

2.2. Coulomb Counting (CC)

The following is a statement of SoC dynamics:

$$SoC_{k+1} = SoC_k - \frac{100\,\eta\,I_{bat,k}\,\Delta t}{3600\,Q_{Ah}}. \quad (1)$$

Here, the state of charge is expressed in percent; η is the coulombic efficiency; the battery current is positive during discharge; Δt is the sampling interval in seconds; and the nominal capacity is expressed in ampere-hours [14].

2.3. Extended Kalman Filter (EKF)

The Thevenin-based 1RC equivalent circuit model used to depict the battery's dynamic electrical behavior is shown in Figure 3. An open-circuit voltage source (OCV), an ohmic resistance R_0 that accounts for sudden voltage drops, and a parallel R_1C_1 branch that captures diffusion dynamics and transient polarization effects make up the model. The internal voltage across the RC network and the current load determine the terminal voltage V_t.

https://doi.org/10.3390/engproc2026160027

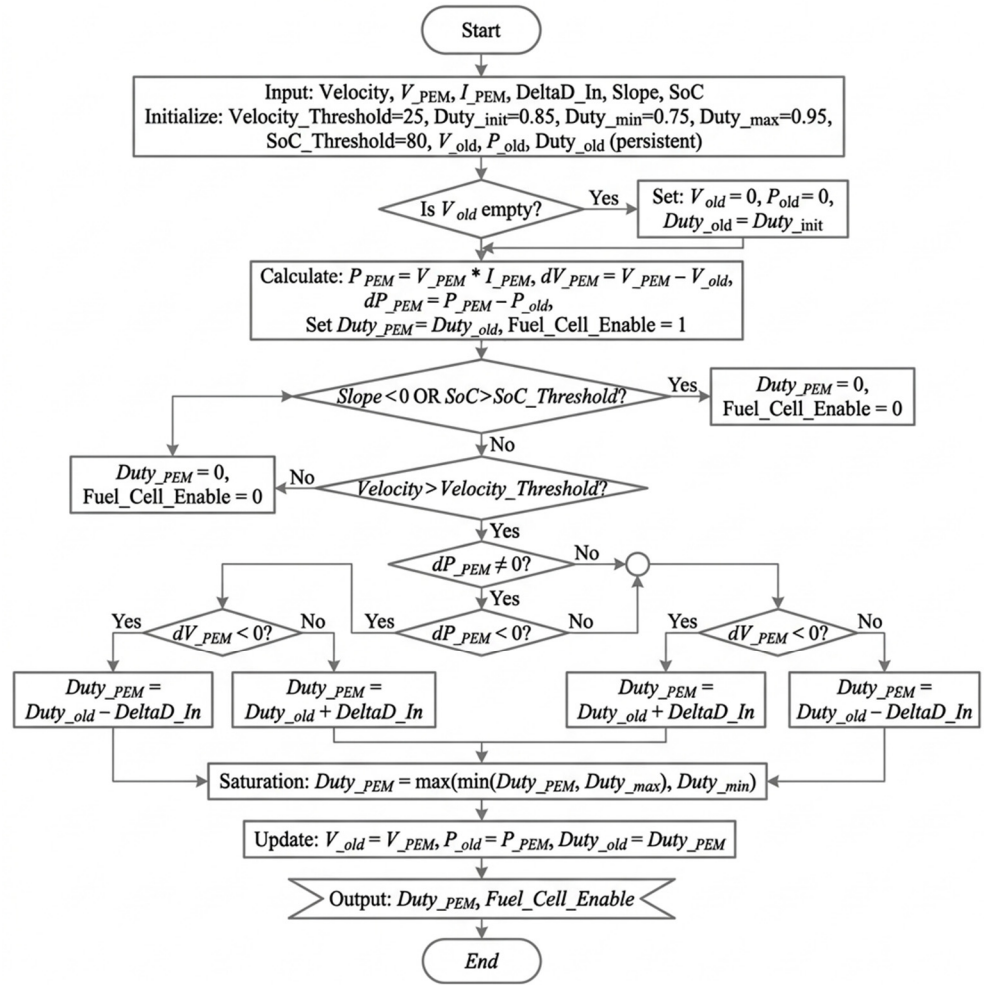


Figure 2. Flowchart of the energy management system.

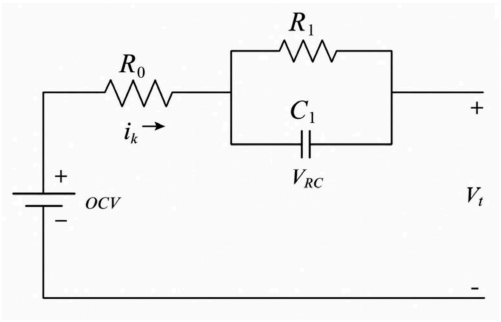


Figure 3. Schematic of the Thevenin 1RC model [15].

A Thevenin-based 1RC equivalent circuit model is used to depict the battery dynamics, with the voltage across the RC network and the state-of-charge serving as the system states. The two states are the battery SoC and the RC-branch polarization voltage. Consequently, the state vector can be written as:

$$x_k = \begin{bmatrix} SoC_k \\ V_{RC,k} \end{bmatrix}. \quad (2)$$

A Coulomb Counting formulation is used to represent the SoC evolution, in which the charge balance is directly controlled by the battery current $I_{bat,k}$. The equation for the discrete-time SoC update is provided by:

$$SoC_{k+1} = SoC_k - \frac{100\,\eta\,I_{bat,k}\,\Delta t}{3600\,Q_{Ah}}. \tag{3}$$

The same SoC convention as in Equation (1) is retained so that the Coulomb Counting and EKF formulations use identical current, capacity, efficiency, time, and percentage conventions. A first-order discrete-time model of the voltage across the RC network is obtained from the continuous-time circuit equation:

$$V_{RC,k+1} = \exp\left(-\frac{\Delta t}{R_1 C_1}\right) V_{RC,k} + R_1\left[1 - \exp\left(-\frac{\Delta t}{R_1 C_1}\right)\right] I_{bat,k}. \tag{4}$$

R_1 and C_1 are the resistance and capacitance of the polarization branch, respectively. The exponential term is the exact zero-order-hold discretization of the first-order RC dynamics over Δt.

Because of the SoC-dependent open-circuit voltage characteristic, the terminal voltage measurement equation is nonlinear and can be written as:

$$V_{bat,k} = OCV(SoC_k) - R_0 I_{bat,k} - V_{RC,k} + v_k. \tag{5}$$

In Equation (5), the terminal-voltage model contains the SoC-dependent open-circuit voltage, the ohmic voltage drop, the RC-branch polarization voltage, and an additive measurement-noise term whose variance is v_k.

$$\hat{x}_{k|k-1} = f\left(\hat{x}_{k-1|k-1}, u_{k-1}\right). \tag{6}$$

The left-hand side is the a priori state estimate. The function $f(\cdot)$ is the nonlinear state-transition model defined by the SoC and RC dynamics, and the input vector includes the battery current. The EKF prediction process is formulated in Equation (6).

$$P_{k|k-1} = A_{k-1} P_{k-1|k-1} A_{k-1}^T + Q_k. \tag{7}$$

In Equation (7), the left-hand side is the a priori estimation-error covariance matrix; A is the state-transition Jacobian evaluated at the previous corrected state; and Q_k is the process noise covariance matrix.

$$H_k = \left.\frac{\partial h(x, u_k)}{\partial x}\right|_{x=\hat{x}_{k|k-1}} = \left[\left.\frac{d\,OCV}{d\,SoC}\right|_{\hat{SoC}_{k|k-1}} \quad -1\right]. \tag{8}$$

Equation (8) defines the measurement Jacobian matrix corresponding to the terminal voltage equation. The measurement Jacobian is obtained by differentiating the terminal-voltage measurement function with respect to the state vector and evaluating it at the predicted state. For the 1RC model, its entries are the local OCV–SoC slope and -1.

$$K_k = P_{k|k-1} H_k^T \left(H_k P_{k|k-1} H_k^T + R_k\right)^{-1}. \tag{9}$$

The Kalman gain is calculated in Equation (9), determining the weighting applied to the measurement during correction, where R_k denotes the measurement-noise variance.

https://doi.org/10.3390/engproc2026160027

The predicted terminal voltage is obtained from the nonlinear measurement model; the difference between measured and predicted terminal voltage is the measurement residual.

$$\hat{x}_{k|k} = \hat{x}_{k|k-1} + K_k\left(V_{bat,k} - V_{pred,k}\right). \quad (10)$$

Equation (10) updates the predicted state vector by incorporating the voltage residual.

$$P_{k|k} = (I_2 - K_k H_k)P_{k|k-1}. \quad (11)$$

The estimation error covariance is refined after the correction step as shown in Equation (11).

$$S\hat{o}C_{k|k} \leftarrow \min\left(100, \max\left(0, S\hat{o}C_{k|k}\right)\right). \quad (12)$$

Equation (12) ensures that the estimated SoC remains within the valid range of 0 to 100%.

Table 1 lists the battery models and the corresponding EKF parameters employed for State-of-Charge (SoC) estimation.

Table 1. Battery model and EKF parameters used for SoC estimation.

Parameter	Description	Value
Ah	Battery capacity	15 Ah
R_0	Ohmic resistance	0.2 Ω
R_1	RC branch resistance	0.01 Ω
C_1	RC branch capacitance	2000 F
Δt	Sampling time	20 ms
$Q_k(1,1)$	SoC process noise variance	10^{-6}
$Q_k(2,2)$	Polarization voltage process noise variance	10^{-4}
R_k	Measurement noise variance	10

3. Results

The comparative results obtained using the Kalman Filter-based and Coulomb Counting-based SoC estimation methods indicate that the influence of the estimation approach on overall vehicle-level performance is limited, whereas its effect on internal energy management behavior is more pronounced. As illustrated in Figures 4–6, the speed-tracking error remains relatively small for both methods throughout the WLTP driving cycle, and the two profiles exhibit a highly similar trend, indicating that the choice of SoC estimation method does not significantly affect speed-following capability.

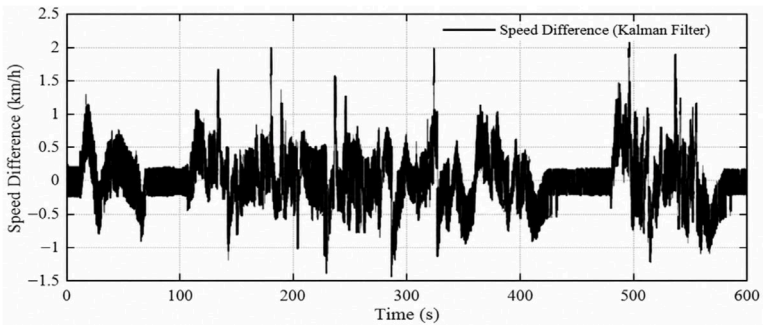


Figure 4. Speed-tracking error obtained with the EKF-based EMS.

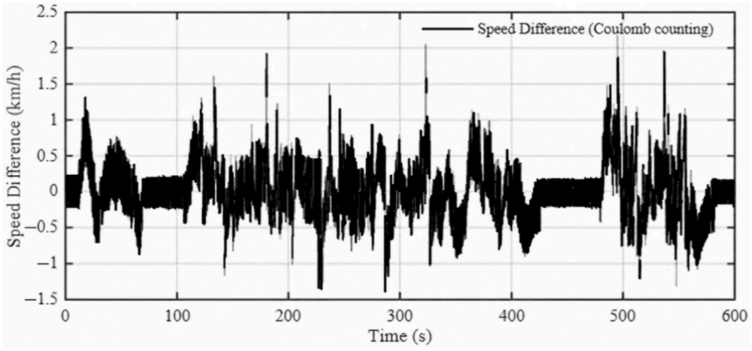


Figure 5. Speed-tracking error obtained with the Coulomb Counting-based EMS.

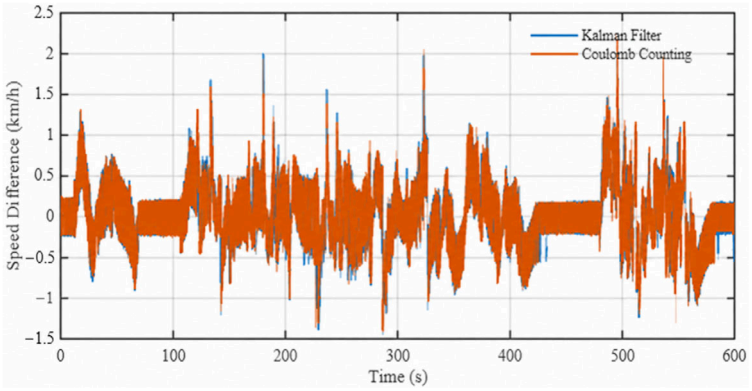


Figure 6. Speed tracking comparison under Kalman Filter-based and Coulomb Counting-based estimation.

A similar observation can be made for the mechanical power demand shown in Figure 7, where the overall power profiles are closely matched, although short-duration deviations appear during rapid transient operating regions. In contrast, the fuel cell power responses presented in Figures 8 and 9 reveal clearer discrepancies between the two methods, particularly during switching intervals and high-demand periods, suggesting that SoC estimation directly affects fuel cell activation and power allocation decisions within the EMS.

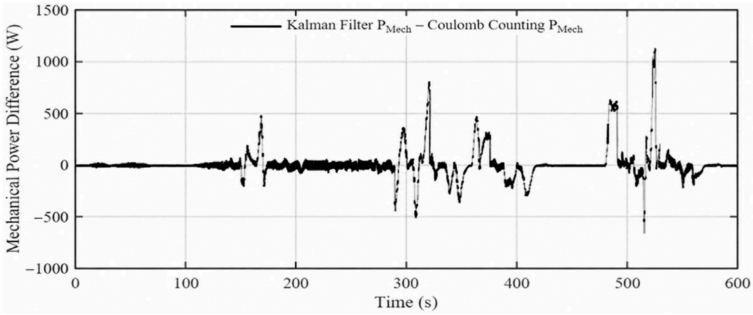


Figure 7. Difference in mechanical power estimates.

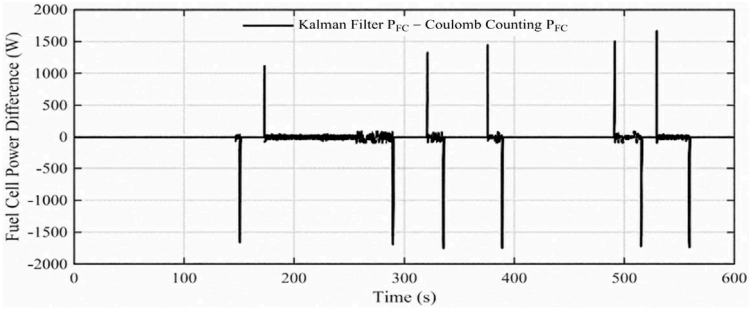


Figure 8. Fuel cell power estimates difference.

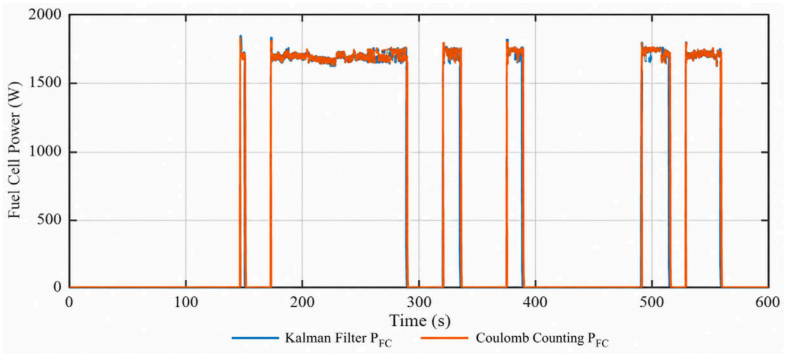


Figure 9. Comparison of fuel cell power estimates.

Likewise, the battery power profiles in Figures 10 and 11 remain generally similar in overall trend, yet noticeable local differences emerge during load transitions and peak demand intervals.

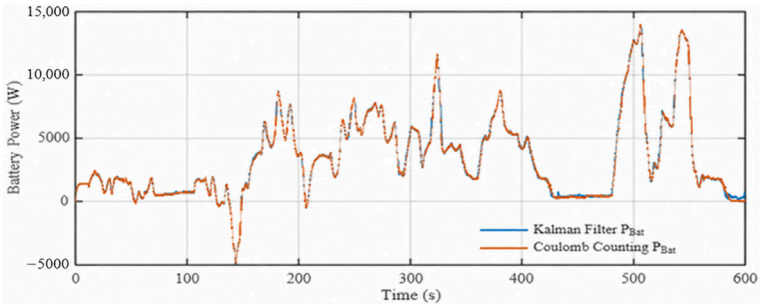


Figure 10. Comparison of battery power estimates.

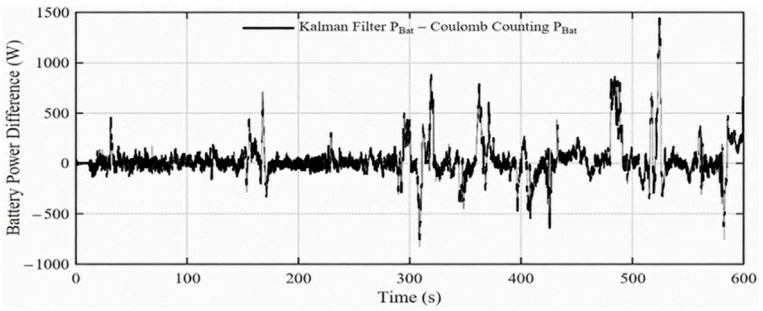


Figure 11. Difference between battery power estimates.

The difference in calculated powers with Kalman Filter and Coulomb Counting-based SoC estimation is shown in Figure 11. However, noticeable differences appear in high-demand regions and transition periods. The difference plot indicates that the

SoC estimation method affects the battery power command, although the overall trend remains similar.

The most distinct divergence is observed in the SoC trajectories shown in Figures 12 and 13, where the Kalman Filter produces a more dynamic and lower SoC profile, while the Coulomb Counting method yields a smoother and consistently higher estimation. These findings demonstrate that although both estimation methods provide comparable vehicle performance in terms of speed tracking and mechanical demand, the selected SoC estimation technique substantially influences the internal power-sharing behavior of the hybrid system and, consequently, the EMS decision-making process.

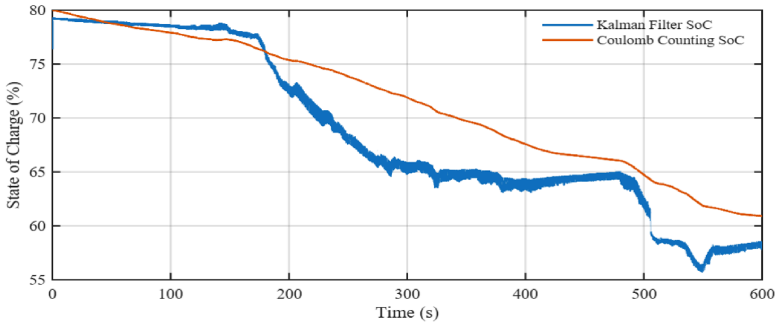


Figure 12. Comparison of SoC profiles obtained using Kalman Filter-based and Coulomb Counting-based estimation.

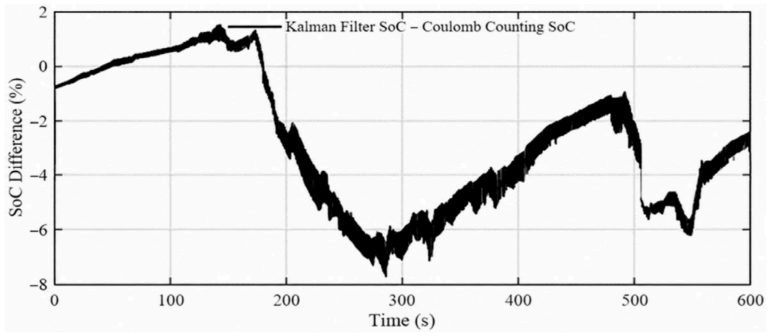


Figure 13. Difference between Kalman Filter-based and Coulomb Counting-based SoC estimates.

Table 2 compares the EMS outputs obtained with Kalman Filter-based and Coulomb Counting-based SoC estimation under the same drive cycle and EMS control.

Table 2. Comparison of EMS outputs obtained using EKF-based and Coulomb Counting-based SoC estimation.

Parameter	Kalman	Coulomb Counting
Final SoC (%)	58.075	60.902
Minimum SoC (%)	55.737	60.902
Maximum SoC (%)	79.249	80.000
SoC Standard Deviation (%)	6.1754	5.1088
Mean Battery Power P_{Bat} (W)	5732.3	5727.7
Standard Deviation of P_{Bat} (W)	3450.7	3458.4
Maximum Absolute P_{Bat} (W)	13,952	13,960
Mean Fuel Cell Power P_{FC} (W)	1507.0	1508.2
Standard Deviation of P_{FC} (W)	551.21	551.56
Maximum Absolute P_{FC} (W)	1845.9	1842.1
Fuel Cell Energy Supplied (Wh)	94.475	94.545
Speed MAE (km/h)	0.29652	0.29708
Speed RMSE (km/h)	0.38879	0.39107

https://doi.org/10.3390/engproc2026160027

Although the EKF and CC configurations produced nearly identical vehicle-level performance, their internal SoC trajectories diverged. Compared with CC, the EKF yielded a 2.827 percentage point lower final SoC and a 5.165 percentage point lower minimum SoC. In addition, the standard deviation of SoC increased by approximately 20.88%, indicating a more dynamically varying internal state estimate. The absolute differences between the two configurations were only 4.6 W in mean battery power, 0.070 Wh in fuel-cell energy supplied, and 0.00228 km/h in speed RMSE, corresponding to relative differences of approximately 0.08%, 0.07%, and 0.58%, respectively. Therefore, the estimator primarily modifies the internal battery state perceived by the EMS rather than the overall traction response. This behavior can be attributed to the rule-based EMS structure: vehicle speed tracking is mainly determined by the traction power demand, whereas SoC affects the timing of fuel cell activation and the local battery/fuel cell power split.

4. Conclusions

In this study, the effects of two different state-of-charge (SoC) estimation methods, namely Coulomb Counting and Extended Kalman Filter, were investigated for a PEM fuel cell/battery hybrid electric vehicle under the same drive cycle and energy management strategy. The results showed that the SoC estimation method had only a limited effect on vehicle-level outputs such as speed tracking and mechanical power demand. Both methods provided very similar speed error characteristics and overall power demand responses. However, more noticeable differences were observed in the energy management behavior. In particular, the Kalman Filter-based estimator produced a lower and more dynamically varying SoC profile, whereas the Coulomb Counting method has a smoother and more optimistic SoC. This difference in SoC estimation propagated into the battery and fuel cell power sharing. The results suggest that vehicle-level performance remains almost unchanged under both estimation methods, since similar speed tracking and mechanical power responses are obtained. However, the SoC profiles differ significantly, which shows that the internal battery state interpretation is estimator-dependent. As a result, the battery and fuel cell power-sharing behavior of the EMS also becomes sensitive to the selected SoC estimation method.

Author Contributions: Conceptualization, K.N.A. and B.Y.; methodology, K.N.A. and B.Y.; software, K.N.A. and B.Y.; validation, B.Y., S.G. and B.Ç.; visualization, K.N.A., B.Y. and S.G.; writing—original draft preparation, K.N.A., B.Y. and S.G.; writing—review and editing, B.Ç. and S.G. All authors have read and agreed to the published version of the manuscript.

Funding: The conference participation was financially supported by the Scientific and Technological Research Council of Türkiye (TÜBİTAK) under the 2224 A Support Program for Participation in Scientific Events Abroad (2026/2) with 1919B142100376 application number.

Institutional Review Board Statement: Not applicable.

Informed Consent Statement: Not applicable.

Data Availability Statement: The data used and generated during the current study are available from the corresponding author upon reasonable request.

Conflicts of Interest: The authors declare no conflicts of interest.

References

1. Li, B.; Gao, X.; Li, J.; Yuan, C. Life cycle environmental impact of high-capacity lithium ion battery with silicon nanowires anode for electric vehicles. *Environ. Sci. Technol.* **2014**, *48*, 3047–3055. [CrossRef] [PubMed]
2. Azad, F.S.; Rahman, A.; Barman, S.D.; Chowdhury, P.; Ali, M.S.; Farrok, O. Towards efficient energy management systems for electric vehicles: Advances in control techniques and applications. *Energy Convers. Manag. X* **2025**, *28*, 101326. [CrossRef]

3. Mansouri, N.; Mnassri, A.; Nasri, S.; Ali, M.; Lashab, A.; Vasquez, J.C.; Guerrero, J.M. Control and optimization of hydrogen hybrid electric vehicles using GPS-based speed estimation. *Electronics* **2025**, *14*, 110. [CrossRef]
4. Sciatti, F.; Tamburrano, P.; Distaso, E.; Amirante, R.; Radogna, A.V.; Morciano, A.; Grassi, G. A comprehensive overview of lithium-ion batteries for electric vehicles: Materials, performance, safety, recycling, and emerging technologies. *J. Energy Storage* **2026**, *144*, 119694. [CrossRef]
5. Wallington, T.J.; Woody, M.; Lewis, G.M.; Keoleian, G.A.; Adler, E.J.; Martins, J.R.R.A.; Collette, M.D. Hydrogen as a sustainable transportation fuel. *Renew. Sustain. Energy Rev.* **2025**, *217*, 115725. [CrossRef]
6. Mendez, C.; Contestabile, M.; Bicer, Y. Hydrogen fuel cell vehicles as a sustainable transportation solution in Qatar and the Gulf Cooperation Council: A review. *Int. J. Hydrogen Energy* **2023**, *48*, 38953–38975. [CrossRef]
7. Yıldız, S.; Yildirim, B.; Özdemir, M.T. Enhancing load frequency control and cybersecurity in renewable energy microgrids: A fuel cell-based solution with non-integer control under cyber-attack. *Int. J. Hydrogen Energy* **2024**, *75*, 438–449. [CrossRef]
8. Alpaslan, E.; Karaoğlan, M.U.; Colpan, C.O. Investigation of drive cycle simulation performance for electric, hybrid, and fuel cell powertrains of a small-sized vehicle. *Int. J. Hydrogen Energy* **2023**, *48*, 39497–39513. [CrossRef]
9. Anonto, H.Z.; Hossain, M.I.; Shahriyar, A.; Banik, T.; Shufian, A.; Emon, M.M.H.; Akteruzzaman, M. SOC estimation in electric vehicles: A comparative evaluation of Kalman filter and Coulomb counting methods. In Proceedings of the 2025 IEEE Region 10 Conference (TENCON), Kota Kinabalu, Malaysia, 27–30 October 2025; IEEE: Piscataway, NJ, USA, 2025; pp. 963–967. [CrossRef]
10. Xiao, R.; Hu, Y.; Jia, X.; Chen, G. A novel estimation of state of charge for the lithium-ion battery in electric vehicle without open circuit voltage experiment. *Energy* **2022**, *243*, 123072. [CrossRef]
11. Wang, L.; Zhao, X.; Deng, Z.; Yang, L. Application of electrochemical impedance spectroscopy in battery management system: State of charge estimation for aging batteries. *J. Energy Storage* **2023**, *57*, 106275. [CrossRef]
12. Liu, Y.; Wang, L.; Li, D.; Wang, K. State-of-health estimation of lithium-ion batteries based on electrochemical impedance spectroscopy: A review. *Prot. Control Mod. Power Syst.* **2023**, *8*, 41. [CrossRef]
13. Yilmaz, B.; Colpan, C.O. Performance analysis of a small-sized hybrid vehicle on a real-world inclined route under WLTP, ARTEMIS, and NEDC drive cycles. *Fuel Cells* **2026**, *26*, e70073. [CrossRef]
14. Dong, J.; Wang, R.; Wang, H.; Hua, S.; Geng, G.; Jiang, Q. Adaptive SOC estimation of grid-level BESS for multiple operational scenarios. *J. Energy Storage* **2025**, *132*, 117776. [CrossRef]
15. He, H.; Qin, H.; Sun, X.; Shui, Y. Comparison study on the battery SoC estimation with EKF and UKF algorithms. *Energies* **2013**, *6*, 5088–5100. [CrossRef]

Disclaimer/Publisher's Note: The statements, opinions and data contained in all publications are solely those of the individual author(s) and contributor(s) and not of MDPI and/or the editor(s). MDPI and/or the editor(s) disclaim responsibility for any injury to people or property resulting from any ideas, methods, instructions or products referred to in the content.